



Letter

Formation of melt-extracted wire of Fe–Cu–Si–B alloy with core-wire/surface-cover-layer structure by arc-melt-type melt-extraction method

Takeshi Nagase^{a,b,*}, Yukichi Umakoshi^c

^a Research Center for Ultra-High Voltage Electron Microscopy, Osaka University, Ibaraki 567-0047, Japan

^b Division of Materials and Manufacturing Science, Graduate School of Engineering, Osaka University, Suita 565-0821, Japan

^c National Institute for Materials Science, 1-2-1 Sengen, Tsukuba, 305-00471, Japan

ARTICLE INFO

Article history:

Received 25 November 2009

Received in revised form 18 January 2010

Accepted 22 January 2010

Available online 2 February 2010

Keywords:

Rapid solidification

Metallic glass

ABSTRACT

A rapidly solidified wire of Fe–Cu–Si–B alloy with a macroscopically separated structure was formed by the arc-melt-type melt-extraction method. A unique core-wire/surface-cover-layer structure composed of core Fe–Si–B-based amorphous alloy and cover Cu crystal was formed by liquid phase separation during rapid quenching of thermal melt.

© 2010 Elsevier B.V. All rights reserved.

1. Introduction

It is important to enhance material processing methods in order to develop new materials with superior structural and functional properties, since these materials can contribute to the sustainable development of human society and maintenance of the global environment. The rapid solidification technique is of considerable interest for the development of new materials. Rapid solidification involves amorphous phase formation, change in the phase selection and solidification mode, liquid phase separation, suppression of segregation, etc. Recently, two-phase amorphous alloys such as La–Zr–Al–Ni–Cu [1], Y–Ti–Al–Co [2], and Ni–Nb–Y [3] have been obtained through liquid phase separation and amorphous phase formation by means of a conventional single-roller melt-spinning method. During the rapid solidification of a multicomponent alloy system, phase separation in a liquid state occurs first, after which each liquid region undergoes a liquid-to-glass transition, resulting in the formation of a new type of metallic material called a two-phase amorphous alloy.

The Fe–Cu alloy system shows a metastable liquid miscibility gap below the liquidus [4–6] because of the demixing component of the Fe–Cu atom pair. Simultaneous liquid phase separation

and amorphous phase formation have been reported in Fe–Cu-based alloys such as the Fe–Cu–Si–B alloy prepared by the rotation water atomizing (RWA) method [7] and the Fe–Cu–Ni–Si–Sn–B–Y [8] and Fe–Cu–Zr–B alloys prepared by the melt-spinning (MSP) method [9,10]. Of the several rapid solidification techniques, the arc-melt-type melt-extraction method yields continuous metallic glass wire [11,12]. In this paper, we report the preparation of a rapidly solidified wire of the Fe–Cu–Si–B alloy by the arc-melt-type melt-extraction method and the formation of a unique core-wire/surface-cover-layer structure through liquid phase separation and amorphous phase formation. To the best of our knowledge, this is the first time such a rapidly solidified wire was prepared.

2. Experimental procedure

The microstructure of the rapidly solidified (Fe₇₅Si₁₀B₁₅)₇₀Cu₃₀ alloy was investigated in this study. As mentioned earlier, the Fe₇₅Si₁₀B₁₅ exhibits the standard alloy composition of the melt-spun amorphous phase former Fe-based alloy [13]. The ratio of Fe–Si–B to Cu was selected as 70–30 on the basis of a previous study that involved simultaneous liquid phase separation and amorphous phase formation during rapid solidification [9]. Master ingots of (Fe₇₅Si₁₀B₁₅)₇₀Cu₃₀ alloy were prepared from Fe, Cu, Si, B, and ferro-boron by means of arc-melting under purified Ar atmosphere on a water-cooled copper substrate. Melt-extracted wire was prepared from the ingots by the arc-melt-type melt-extraction method [11,12]. Fig. 1 shows (a) a schematic illustration and (b) the corresponding image of the apparatus (NISSIN-GIKEN, NEV-AT3). The diameter of the Cu roll used in this method was 200 mm, and the angle of the edge was fixed at 60°. The rotation speed was maintained at 1000 rotations per minute (rpm) or 2000 rpm, and the circumferential velocity of the Cu roll was 21 ms⁻¹ at 2000 rpm. Mother alloys were arc-melted from the master ingots under Ar gas atmosphere on a water-cooled Cu mold. This apparatus allowed us to control the position of the Cu roll. The molten mother alloy was extracted by moving

* Corresponding author at: Research Center for Ultra-High Voltage Electron Microscopy, Osaka University, 7-1 Mihogaoka, Ibaraki 567-0047, Japan. Tel.: +81 6 6879 7941; fax: +81 6 6879 7942.

E-mail address: t-nagase@uhvem.osaka-u.ac.jp (T. Nagase).

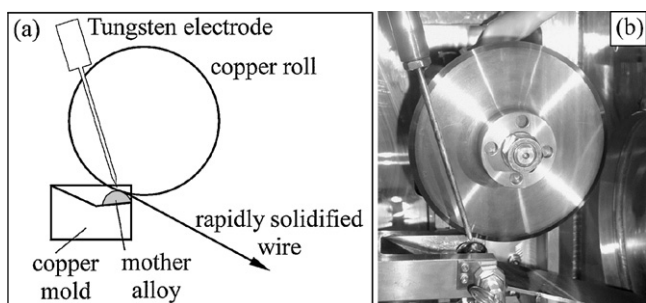


Fig. 1. Schematic illustration of arc-melt-type melt-extraction method used in this study. (a) Schematic illustration of the method and (b) photograph of the apparatus.

down the rotating Cu roll. The lower the rotation speed, the larger is the diameter of the melt-extracted wire. In the present study, the melt-extracted wire prepared at 2000 rpm was investigated in detail. For comparison purposes, melt-spun ribbon was also prepared by the conventional single-roller melt-spinning method. The structure of the melt-spun ribbon was examined by X-ray diffractometry (XRD) using Cu K α radiation, an optical microscope (OM), a back electron scattering X-ray image (BEI) obtained by scanning electron microscopy (SEM), an electron-probe micro-analyzer (EPMA), and differential scanning calorimetry (DSC) at a heating rate of 0.67 K s $^{-1}$ in Ar atmosphere.

3. Results and discussion

Fig. 2 shows the outer appearance of a melt-extracted wire of the (Fe $_{75}$ Si $_{10}$ B $_{15}$) $_{70}$ Cu $_{30}$ alloy. A continuous wire can be prepared by the arc-melt-type melt-extraction method. **Fig. 2(b)** and **(c)** shows the magnified images of the melt-extracted wire shown

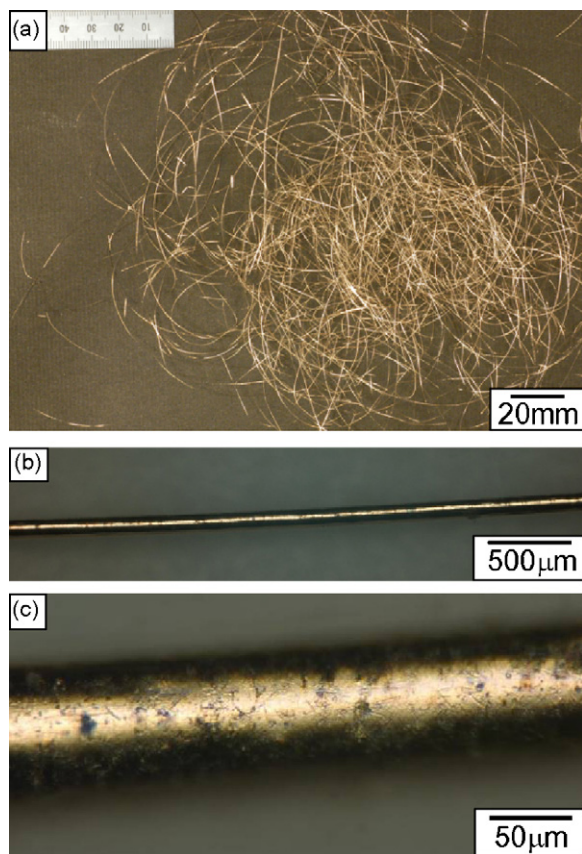


Fig. 2. Outer appearance of melt-extracted wire of (Fe $_{75}$ Si $_{10}$ B $_{15}$) $_{70}$ Cu $_{30}$ alloy. (b) and (c) show the magnified images of (a). A copper-colored surface is observed instead of the metallic silver-colored surface that is characteristic of conventional metallic materials. (For interpretation of the references to color in this figure legend, the reader is referred to the web version of the article.)

in **Fig. 2(a)**. It can be observed that the wire does not show a metallic silver-colored surface that is characteristic of conventional metallic materials but a copper-colored surface. Fluctuations in the diameter cannot be observed in **(b)**, indicating that the melt-extraction method is very effective in preparing the rapidly quenched wire with high-quality morphology. From **Fig. 2(c)**, it can be observed that the Fe–Cu–Si–B alloy has a slightly rough surface and not a mirror surface that is characteristic of melt-extracted amorphous wires [12].

The constituent phases of the melt-extracted Fe–Cu–Si–B wire were investigated using XRD analysis and DSC measurement. **Fig. 3(a)** shows the XRD patterns of melt-extracted alloy wires together with those of the melt-spun ribbon for comparison. The XRD pattern of the melt-spun ribbon shows sharp diffraction peaks corresponding to the fcc-Cu phase and a broad halo ring corresponding to the amorphous phase, and the pattern is similar to that of the rapidly solidified powders prepared by RWA [7] and whose constituent phases are an Fe–Si–B-based amorphous phase and fcc-Cu crystalline phase. In contrast, the melt-extracted wire shows sharp diffraction peaks corresponding not only to the fcc-Cu crystalline phase but also to the bcc-Fe crystalline phase. The shoulder of the diffraction peak can be observed at approximately $2\theta = 47^\circ$. It is very difficult to identify the existence of a broad halo ring in the curve because the position of the broad peak overlaps with the (1 1 0) peak of bcc-Fe. In order to confirm the formation of an amorphous phase in the melt-extracted wire, DSC measurement was performed; the measurement results are shown in **Fig. 3(b)**. The melt-spun ribbon shows two exothermic peaks corresponding to the crystallization of the amorphous phase. The DSC curves and the crystallization temperatures T_{x1} and T_{x2} for the melt-spun ribbon are similar to those for the Fe $_{75}$ Si $_{10}$ B $_{15}$ melt-spun ribbon without Cu [13]; the first broad peak (T_{x1}) corresponds to the precipitation of the bcc-Fe solid solution from the amorphous phase and the second sharp peak (T_{x2}) corresponds to the formation of intermetallic compounds. The constituent phases of the melt-spun ribbon can be considered to be the mixture of the Fe–Si–B-based amorphous phase and Cu crystalline phase. The DSC curve of the melt-extracted wire shows one exothermic peak at the crystallization temperature T_{x3} . T_{x3} is similar to T_{x2} , whereas the exothermic heat release at T_{x3} is smaller than that at T_{x2} . The exothermic reaction at T_{x3} can be considered to correspond to that at T_{x2} ; the melt-extracted wire contains an amorphous phase, and crystallization of this amorphous phase for the formation of intermetallic compounds was observed in the DSC analysis. The exothermic peak at T_{x1} cannot be observed for the melt-extracted wire, indicating that the bcc-Fe phase was already formed during the rapid quenching of the thermal melt because of the lower cooling rate in the melt-extraction method than in the melt-spinning method. XRD and DSC curves show the formation of the Fe–Si–B-based amorphous phase together with the formation of the fcc-Cu and bcc-Fe crystalline phases in the melt-extracted wire.

Fig. 4 shows the SEM–BEI of the microstructure of the melt-extracted wire and the melt-spun ribbon in the Fe–Cu–Si–B alloy. The inner region of the melt-spun ribbon shown in **Fig. 4(a)** shows an emulsion structure similar to that observed in the SEM image of rapidly solidified powder [9]; the white circular fcc-Cu crystalline phase is embedded in the gray Fe–Si–B amorphous matrix. **Fig. 4(b)** shows the SEM–BEI image observed in a direction perpendicular to the wire direction. The melt-extracted wire exhibits a macroscopically separated structure. The inner region of the wire shows a gray contrast with small white circular globules, whereas the outer surface region of the wire shows a white contrast, indicating the formation of a core-wire/surface-cover-layer structure. **Fig. 4(c)** shows the magnified image of the melt-extracted wire. It shows the emulsion structure formation both in the gray matrix region of the inner core-wire and in the white region of the outer surface-cover layer.

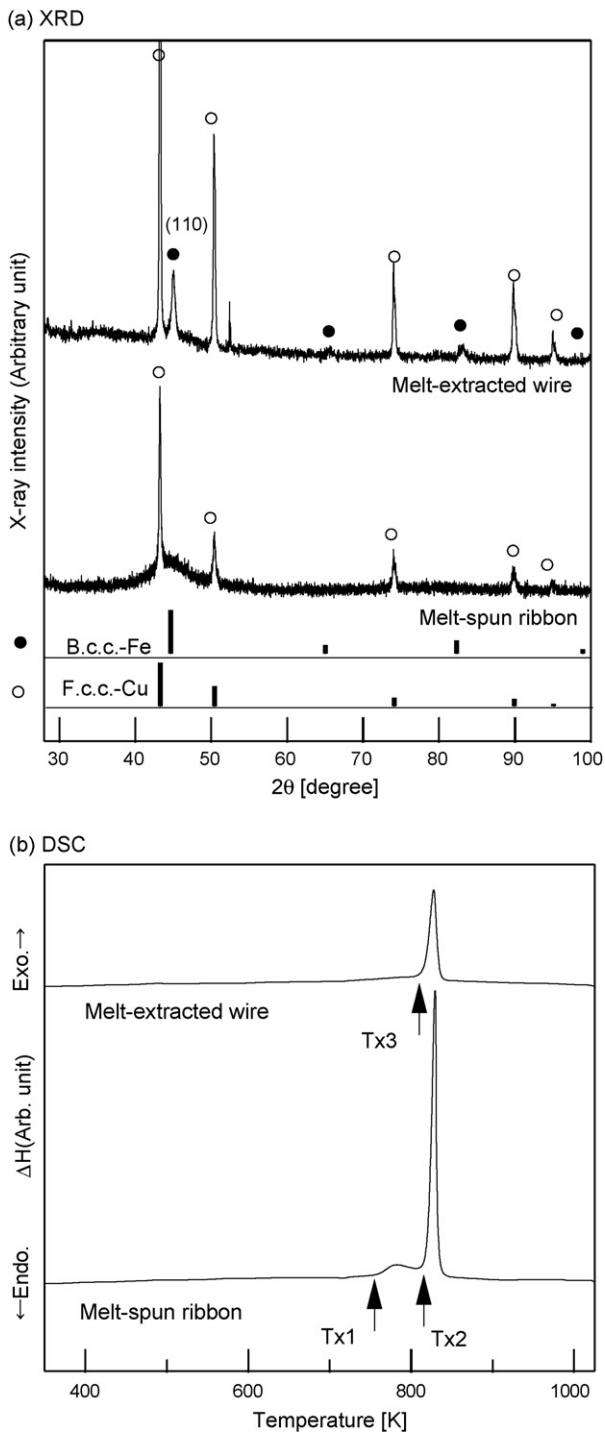


Fig. 3. XRD patterns (a) and DSC curves (b) of melt-extracted wire and melt-spun ribbon of $(\text{Fe}_{75}\text{Si}_{10}\text{B}_{15})_{70}\text{Cu}_{30}$ alloy.

The SEM–BEI structure of the inner core-wire region is similar to that of the melt-spun ribbon. The interface of the inner core-wire region and the outer surface-cover-layer region is very smooth; this is characteristic of the structure obtained through liquid phase separation. In order to investigate the microstructure of the melt-extracted wire in detail, EPMA analysis was performed. The results are shown in Fig. 5; for (a)–(e), the observation direction is perpendicular to the wire direction, whereas (f)–(j) are cross-sectional images. The inner core-wire region contains Fe, Si, and B, whereas the outer surface-cover layer mainly contains Cu. The formation of an Fe–Si–B-based alloy core-wire/Cu-rich alloy surface-cover layer

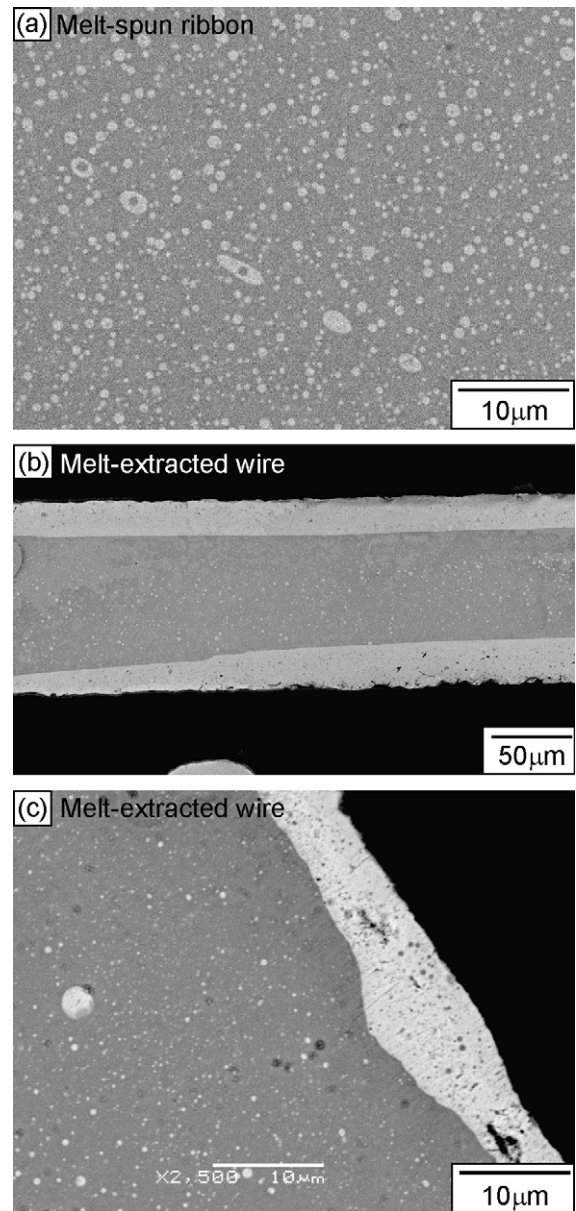


Fig. 4. Back electron scattering image (BEI) of SEM microstructure of melt-extracted wire and melt-spun ribbon of $(\text{Fe}_{75}\text{Si}_{10}\text{B}_{15})_{70}\text{Cu}_{30}$ alloy. (a) Melt-spun ribbon and (b) and (c) melt-extracted wire.

in the melt-extracted wire was confirmed by SEM and EPMA analysis. The copper color in the melt-extracted wire was attributed to the formation of the fcc-Cu crystal surface-cover layer. The inner core-wire region contains fcc-Cu globules that show a white circular contrast, and the outer surface-cover-layer region contains Fe–Si–B-based alloy globules that show a gray circular contrast. The globule formation is attributed to the liquid phase separation of the Fe–Si–B-based alloy liquid and Cu-rich liquid. The inner core-wire Fe–Si–B alloy region also shows a fluctuation in the Fe and Si compositions. This might be due to the precipitation of the bcc-Fe phase and/or intermetallic compounds because of crystallization of the Fe–Si–B amorphous and/or liquid phase. No significant difference could be observed in macroscopically separated core-wire/surface-cover-layer structure formation and the microstructure of the melt-extracted wire between 2000 rpm and 1000 rpm. The reason for the formation of the unique core-wire/surface-cover-layer structure is not clear; however, the following mechanism can be considered. Wang et al. reported that an egg-like structure formed

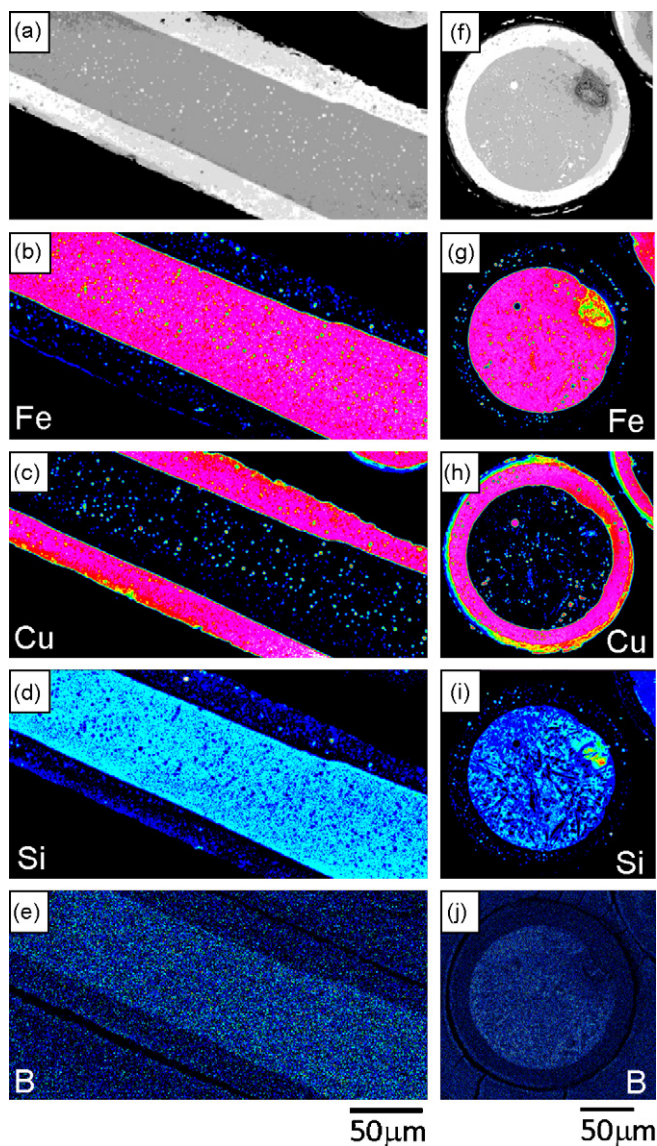


Fig. 5. EPMA-WDX analysis of melt-extracted wire in $(\text{Fe}_{75}\text{Si}_{10}\text{B}_{15})_{70}\text{Cu}_{30}$ alloy. (a)–(e) The observation direction is perpendicular to the wire direction, whereas (f)–(j) cross-sectional images. (a and f) BEI image, (b and g) Fe image, (c and h) Cu image, (d and i) Si image, and (e and j) B image.

in the Cu–Fe–Si–C alloy atomized powders was composed of Fe-rich core crystalline phases and a Cu-rich surface layer [14], and the difference in the surface energy and the rotation of drops induced by the extremely rapid gas flow in the atomization process were the important factors affecting the formation of the egg-like structure. The difference between the surface energies of the Fe–Si–B-rich and Cu-rich alloy liquids and the Marangoni motion of the liquids may be the important factors affecting the formation of the core-wire/surface-cover layer in the melt-extracted wire. During the free flight of thermal melt, the liquid phase separation of the Fe–Si–B-based liquid and Cu-rich liquid occurs first, which is followed by the aggregation of both liquids, resulting in the formation of macroscopically separated structures. The formation of the

Fe–Si–B amorphous phase indicates that the Fe–Si–B liquid maintains its liquid structure at the glass transition temperature during the cooling of thermal melt, resulting in the maintenance of the liquid state enough to the formation of macroscopically liquid phase separation structure.

It is well known that Fe–Si–B amorphous alloys are high-quality and low-cost soft magnetic materials [15–17]. Heat release from soft magnetic materials is an important factor for the use of magnetic devices. The thin Cu layer of the melt-extracted wire may be effective for the use of this alloy as a soft magnetic material because of the high thermal conductivity of Cu and the closely attached interface without any interrupting elements such as oxides and/or voids between the Cu surface layer and the Fe–Si–B core wire.

4. Conclusion

In the present study, a rapidly solidified Fe–Cu–Si–B wire was prepared by the arc-melt-type melt-extraction method. The following conclusions were obtained:

- (1) A continuous wire of Fe–Cu–Si–B alloy with a very smooth surface and negligible fluctuation in diameter can be prepared by the arc-melt-type melt-extraction method.
- (2) The rapidly solidified wire shows an Fe–Si–B-based amorphous alloy core-wire/fcc-Cu crystalline surface-cover-layer structure obtained through liquid phase separation and an amorphous phase formation.

Acknowledgements

This work was supported by a Grant-in-Aid for Scientific Research on Priority Area A, “Materials Science of Metallic Glasses” from the Ministry of Education, Culture, Sports, Science and Technology (MEXT) of Japan. A part of this work was also supported by Priority Assistance for the Formation of Worldwide Renowned Centers of Research—The Global COE Program (Project: Center of Excellence for Advanced Structural and Functional Materials Design).

References

- [1] A.A. Kundig, M. Ohnuma, D.H. Ping, T. Ohkubo, K. Hono, *Acta Mater.* 52 (2004) 2441–2448.
- [2] B.J. Park, H.J. Chang, D.H. Kim, W.T. Kim, *Appl. Phys. Lett.* 85 (2004) 6353–6355.
- [3] N. Mattern, U. Kuhn, A. Gebert, T. Gemming, M. Zinkevich, H. Wendrock, L. Schultz, *Scripta Mater.* 53 (2005) 271–274.
- [4] Y. Nakagawa, *Acta Metall.* 6 (1958) 704–711.
- [5] K. Iwase, M. Okamoto, T. Amemiya, *Sci. Rep. Tohoku Univ.* 14 (1937) 618–640.
- [6] P.A. Kindqvist, B. Uhrenius, *Calphad* 4 (1980) 193–200.
- [7] I. Yamauchi, T. Irie, H. Sakaguchi, *J. Alloys Compd.* 403 (2005) 211–216.
- [8] T. Koziel, Z. Kedzierski, A. Zielinska-Lipiec, K. Ziewiec, *Scripta Mater.* 54 (2006) 1991–1995.
- [9] T. Nagase, A. Yokoyama, Y. Umakoshi, *Mater. Trans.* 47 (2006) 1105–1114.
- [10] T. Nagase, A. Yokoyama, Y. Umakoshi, *J. Alloys Compd.*, in press.
- [11] H. Kimura, A. Inoue, K. Sasamori, H. Ohtsubo, Y. Waku, *Jpn. Soc. Powder Powder Metall.* 47 (1999) 427–432.
- [12] T. Nagase, K. Kinoshita, Y. Umakoshi, *Mater. Trans.* 49 (2008) 1385–1394.
- [13] A. Inoue, T. Masumoto, M. Kikuchi, T. Minemura, *Sci. Rep. RITU A-27* (1979) 126–146.
- [14] C.P. Wang, X.J. Liu, I. Ohnuma, R. Kainuma, K. Ishida, *Science* 297 (2002) 990–993.
- [15] Collected Abstracts of the 1975 Meeting of the Japan Inst. Metals, 1975, pp. 341.
- [16] T. Masumoto, K. Fukamichi, *Amorphous Alloys*, Agne, Tokyo, 1981.
- [17] Metglas, Inc.: 2605SA1 Alloy Technical Bulletin, 1981.